The Circuit Model for Electro-Quasistatic Human Body Communication

Lingke Ding, *Student Member, IEEE* and Shreyas Sen, *Senior Member, IEEE*
Elmore Family School of Electrical and Computer Engineering, Purdue University, West Lafayette, USA
E-mail: ding359@purdue.edu, shreyas@purdue.edu

***Abstract*—This paper comprehensively reviews the evolution of Electro-Quasistatic (EQS) Human Body Communication (HBC) circuit models for wireless on-body communication and powering. As the Internet of Bodies (IoB) rapidly advances, driven by innovations in communication, security, and computing, HBC has emerged as a key technology offering high-speed, low-power data transmission through the body itself. This approach promises reliable communication and the potential for perpetual nodes via ultra-low-power operation and energy harvesting. Building on the foundational IoB vision established in prior work, we consolidate key insights from recent developments in HBC circuit modeling, with an emphasis on understanding the human body as a communication and power transfer medium. The review covers both capacitive and galvanic EQS-HBC models, analyzing the role of parasitic capacitance and the transition conditions between unsymmetrical galvanic and capacitive modes. We also discuss future opportunities and challenges in resonant-HBC, which enables higher data rates. This work provides a structured foundation for advancing low-power, secure, and scalable body-centric communication systems.**

***Index Terms*—Human Body Communication, Internet of Bodies, Biophysical Modeling**

I. Introduction

Wearable technologies are increasingly essential in various impactful applications, such as augmented/virtual reality glasses, remote healthcare monitoring, and fitness tracking, enabling continuous sensing, immersive experiences, and real-time physiological data collection. As demand for wearable devices grows, so does the need for efficient, low-power communication systems capable of supporting high-speed, all-day-long data transmission. Electro-Quasistatic (EQS) Human Body Communication (HBC) has emerged as a promising solution, using the body itself as a transmission medium to enable reliable, ultra-low-power communication for wearables, potentially supporting perpetual operation of such nodes [1]. Building on the foundational vision of the Internet of Bodies (IoB) paradigm established in our prior work [2], this review paper summarizes recent progress in understanding the human body circuit model for enabling both wireless on-body communication and powering. We focus on consolidating key circuit models and insights that enable low-power, secure, and scalable HBC systems, providing a structured reference point for future research and application development.

Unlike traditional wireless technologies that utilize air as the transmission medium, HBC takes advantage of the high water content within the human body to provide a low-loss channel for signal propagation [3]. Based on the operating frequency, HBC can be categorized into EQS and resonant modes. In EQS-HBC, signals are largely contained within the human body with minimal leakage into the surroundings [3]–[10]. This creates a secure communication channel, where over-the-air eavesdropping becomes impractical. In contrast, resonant-HBC allows the human body to act as a transmission antenna, enabling higher data rates and lower channel losses, making it suitable for applications with increased data demands [11].

Despite its potential, the field of HBC is still in its early stages. A wide range of research has explored different applications and demonstrated technological viability [3]–[6], [10], [12]–[23], yet a unified consensus on how to model HBC circuits remains elusive. This lack of standardization in modeling has hindered progress and limited the design of HBC systems, which often rely on heuristics. As research into the lumped biophysical behavior of the body channel progresses [11], [24]–[34], there is a pressing need to consolidate and systematize the existing circuit models for HBC. This paper addresses this gap by reviewing and analyzing key circuit models for EQS-HBC, providing a foundation for future circuit-based HBC applications.

The paper is organized as follows: Section II provides the background and key concepts related to HBC. Sections III and IV discuss the circuit model for capacitive EQS-HBC and explain the two critical parasitic capacitors influencing channel performance. Section V introduces galvanic EQS-HBC and explores its similarities to capacitive models. Section VII summarizes the key circuit models presented in this review.

II. Background and Key Concepts

Human Body Communication (HBC) was first introduced by Zimmerman et al. [35] as a low-frequency alternative to near-field communication for personal area networks. The goal of establishing an ubiquitous on-body information network has remained a driving force behind HBC research, as well as the ongoing effort to develop a simplified, yet effective, lumped circuit model that captures the essential characteristics of the channel without becoming overly complex. Such a model is crucial for providing insights into system-level design and optimization.

Early work by Cho et al. approached the body channel as a distributed model composed of resistive and capacitive (RC) elements, where the body was broken down into smaller segments with corresponding electrical properties [24]. Although this RC model captures the distributed nature of the body, it

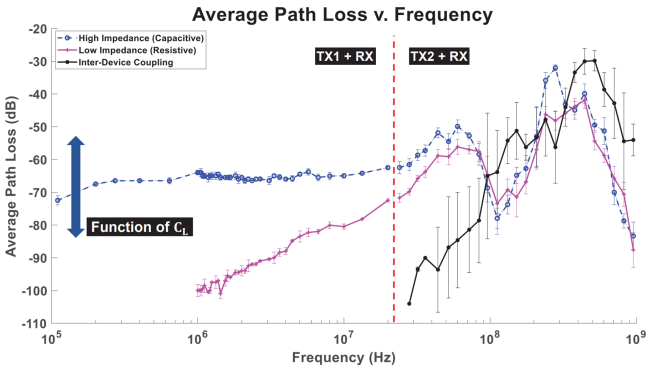

Fig. 1. Measured channel response of capacitive HBC across various frequencies using a wearable transmitter and receiver setup. C_L refers to the input capacitance of the receiver, as shown in Fig. 2. Two TXs were employed to achieve sufficient frequency tunability for sweeping the full frequency spectrum.

proves too complex for practical circuit optimization of the transmitter (TX) or receiver (RX), making it less useful for intuitive system design. To address this issue, Maity et al. and Nath et al. proposed an alternative approach that combines finite element analysis (FEA) with physical experiments to identify the most critical components of the body channel, which can then be represented by a simplified lumped circuit model [25], [26]. While lumped models are less precise than distributed ones, they capture the core behavior of HBC and allow for easier analysis, making them more suitable for optimizing circuit parameters in real-world applications.

In terms of signal transmission, HBC can be classified into two primary modes based on the arrangement of electrodes: capacitive HBC and galvanic HBC. In capacitive HBC, only the signal electrodes of both the TX and RX are in contact with the human body, while the ground electrodes are left floating, forming parasitic capacitors with the environment. Conversely, in galvanic HBC, both the signal and ground electrodes are attached directly to the body, allowing for direct electrical conduction through the body tissues. These differences in electrode configuration lead to different channel characteristics and signal propagation behaviors.

Additionally, HBC can be classified by its operating frequency into two primary modes: EQS and resonant mode. In EQS mode, the transmission signal frequency wavelength is significantly larger than the body channel length. Consequently, the electric field distribution across the body remains nearly constant, leading to the electro-quasistatic designation. In this mode, the human body can be modeled as a lumped element, and with the RX using high impedance termination, the body can be further simplified as an equipotential surface, making circuit analysis more tractable. Conversely, in resonant mode, the signal wavelength is comparable to or shorter than the human body length, causing the body to behave more like a radiative antenna. As shown in Fig. 1 (TX2 + RX region), in this mode, the human body exhibits inductive behavior, which enhances the transmitted signal and results in lower channel losses while supporting higher data rates. The transition between EQS and resonant modes depends on the physical dimensions of the human body. For instance, assuming an average body length of approximately 2 meters, a frequency of 30 MHz with a wavelength of around 10 meters typically marks the boundary between these two modes.

Despite significant progress in understanding HBC, a consensus on optimal circuit models and system-level designs remains elusive. The challenge of balancing modeling accuracy with simplicity leaves much of the design space unexplored. This review addresses this gap by analyzing key circuit models for capacitive and galvanic HBC, offering insights for future circuit-based applications.

III. Biophysical Modeling of Capacitive EQS-HBC

In capacitive EQS-HBC, the signal return path is established as follows: the TX couples the signal onto the body via the signal electrode in contact with the body. The signal then propagates through the body and is sensed by the signal electrode of the RX. From there, the signal travels through the parasitic capacitance formed between the floating RX ground electrode and the environmental ground, and subsequently through the parasitic capacitance formed between the floating TX ground electrode and the environmental ground, completing the return path to the transmitter.

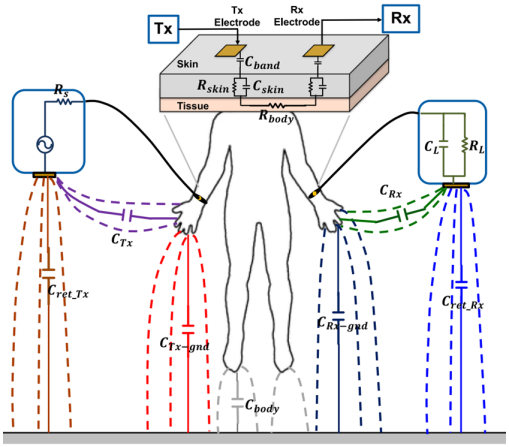

Fig. 2. Detailed lumped circuit model for capacitive EQS-HBC, illustrating the field lines and parasitic capacitances between the electrodes, the body, and the environmental ground.

Maity et al. conducted physical experiments combined with circuit simulations to develop the first lumped biophysical model of the body channel for capacitive EQS-HBC, as shown in Fig. 2 [25]. Given that the operating frequency lies within the EQS range, the distributed behavior of the body channel can be approximated by a single lumped element, predominantly resistive, with parasitic capacitance formed between the body and the environmental ground, denoted as C_{body}. Due to the significantly higher impedance of the outermost layer of the skin compared to the underlying layers of fat, tissue, and conductive fluids, signal propagation primarily occurs

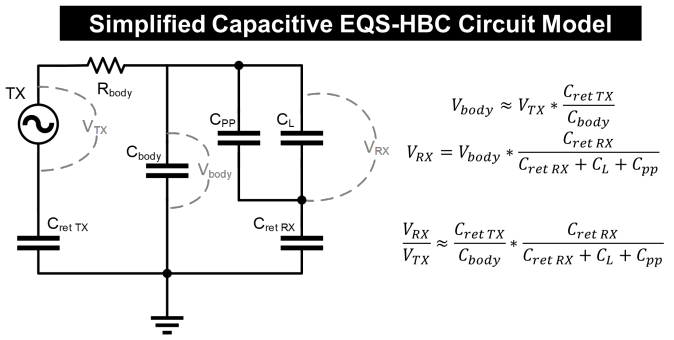

Fig. 3. Simplified circuit model for capacitive EQS-HBC, along with the corresponding channel gain formula, illustrating the most significant circuit components.

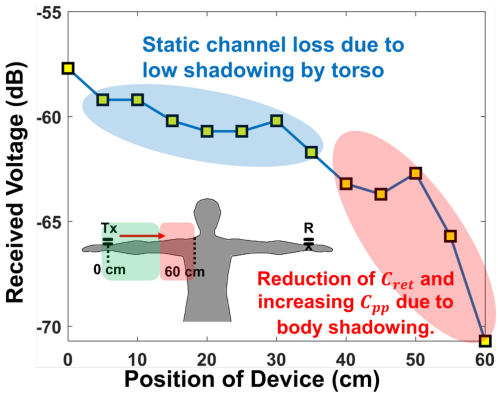

Fig. 4. Measured change in received voltage as the transmitter (TX) is moved from the wrist to the shoulder. The reduction in C_{ret} due to body shadowing and the corresponding increase in C_{pp} lead to a decrease in the received voltage.

through the internal layers of the body. As a result, the contact impedance between the electrode and the skin and the skin impedance are incorporated into the model.

Furthermore, for voltage mode communication, the body tissue impedance, contact impedance, and skin impedance can be combined, leading to a more simplified lumped biophysical model, illustrated in Fig. 3. Maity et al. experimentally determined the return path capacitance (C_{ret}) to be approximately 1.5 pF, with AC impedance exceeding 100 $k\Omega$ at 1 MHz, while the human body tissue impedance is around 100 Ω [25]. Since C_{ret} is in series with the body tissue impedance, its effect is negligible and can be combined with the contact and skin impedance into a single term, denoted as R_{body}. Consequently, the model proposed by Maity et al. is simplified into a configuration comprising four parasitic capacitors and a single resistor, highlighting the key circuit components that determine the channel response [26]. Furthermore, experimental results indicate that even in the absence of $C_{ret\ TX}$ and $C_{ret\ RX}$, the channel loss through the human body is nearly 0dB with high impedance termination, suggesting that the effect of R_{body} can be neglected for capacitive EQS-HBC.

Therefore, the on-body voltage gain from the transmitted voltage could be approximated using this formula:

$$V_{body} \approx V_{TX} \cdot \frac{C_{ret\ TX}}{C_{body}} \tag{1}$$

If the receiver uses capacitive termination of C_L, the received voltage gain to the on-body voltage could be approximated using this formula, C_{pp} will be introduced in the following section:

$$V_{RX} = V_{body} \cdot \frac{C_{ret\ RX}}{C_{ret\ RX} + C_L + C_{pp}} \tag{2}$$

IV. The Parasitic Capacitors

As discussed in the previous section, parasitic capacitances are critical in influencing the channel response in capacitive EQS-HBC. Extensive research has been conducted to examine the two primary sources of parasitic capacitance, C_{ret} and C_{pp}, and their impact on the channel response [26], [29].

The parasitic capacitance C_{ret} is formed between the ground electrode of the TX or RX and the environmental ground. Nath et al. performed a series of experiments, concluding that C_{ret} can be estimated based on the self-capacitance of the ground electrode when the dimensions of the TX or RX are significantly smaller than the distance to the environmental ground [26]. For a wearable device designed as a disc shape with radius r and thickness h, its C_{ret} can be approximated as:

$$C_{ret} = 8\epsilon_0 r \left[1 + 0.87(\frac{h}{2r})^{0.76}\right] \tag{3}$$

For a thin device, when $h << r$,

$$C_{ret} \approx 8\epsilon_0 r \tag{4}$$

When RX is employed as a wearable, the human body together with the device signal electrode forms an additional parasitic capacitance, C_{pp}, with the ground electrode of the device. Parasitic capacitors come from the electric fringe fields extending from the device ground electrode to another conductive element. In the absence of human body, all fringe fields originated from the device ground electrode terminate on the environmental ground, and this is the maximum C_{ret} attainable. In the presence of the human body, which acts as a semi-conductive medium, some fringe fields terminate on the body instead of the environmental ground, as if the body is shadowing part of the ground from the ground electrode. This phenomenon is referred to as the body shadowing effect. As demonstrated by Datta et al., the received voltage decreases significantly when the body shadowing effect is more pronounced, due to a reduction in C_{ret} and a corresponding increase in C_{pp} [29]. In practical applications, areas of low body shadowing effect, such as the wrists, experience less voltage attenuation, whereas regions with high body shadowing effect, such as the neck, exhibit greater voltage reduction (Fig. 4).

V. Biophysical Modeling of Galvanic EQS-HBC

In galvanic EQS-HBC, if the TX and RX are symmetric, where both pairs of the signal and ground electrode possess identical size and shape with equal C_{ret}, the signal transmission path is formed between the TX signal electrode and the

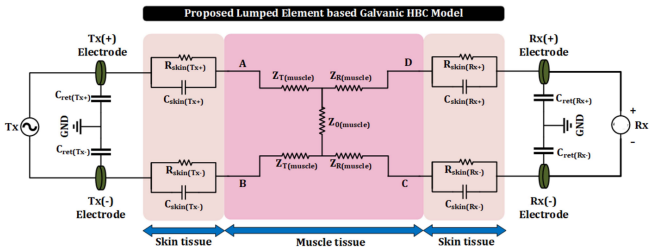

Fig. 5. The simplified circuit model for galvanic EQS-HBC.

TX ground electrode, with the RX operating in parallel along a section of the transmission path. Modak et al. characterized the channel gain function with s as the distance between the signal and ground electrode, d as the distance between the TX electrode pair and RX electrode pair, and θ as the angle between the electrode pairs [30]. The channel gain function is:

$$Gain = 20\log\left[\frac{R_{muscle}}{2R_{skin}}\right] + 10\log\left[\frac{1+(2\pi f C_{skin}R_{skin})^2}{1+(\pi f C_{skin}R_{muscle})^2}\right] + 20\log\left[\left|\frac{\ln\sqrt{(1+\frac{s^2}{d^2})^2-(\frac{2s}{d}sin\theta)^2}}{\ln\frac{s^2}{r^2}}\right|\right] \quad (5)$$

This equation reveals two key insights about the channel response: (1) it is dependent on signal division between the skin and muscle layers, scaled by a constant factor, and (2) it depends on the channel distance, the distance between the signal and ground electrode pairs of TX and RX, and the angular position of the RX relative to the TX. Experimental results show that the channel loss is low over short distances, with loss increasing with length, saturating to a constant value for channel lengths exceeding 50 cm [30].

On the contrary, if the TX and RX are non-symmetric, with signal and ground electrodes differing in size and shape and unequal C_{ret}, the channel response becomes similar to capacitive EQS-HBC, as demonstrated by Modak et al. and illustrated in Fig. 6 [30]. This behavior can be intuitively understood by analyzing Eqn. 1.

In the symmetric case, where the TX signal and ground electrodes are identical in size and shape, the V_{body} contributions from the signal and ground electrodes can be calculated using Eqn. 1. These contributions are equal in amplitude but 180 degrees out of phase, resulting in a net zero voltage summation. However, when the TX signal and ground electrodes are unsymmetrical, V_{body} at the TX signal and ground electrodes remain 180 degrees out of phase but differ in amplitude, producing a non-zero summation. This non-zero voltage is referred to as the common mode voltage. With a common mode voltage on the body, the unsymmetrical galvanic TX begins to behave similarly to a capacitive TX, as it introduces capacitive-like signal propagation characteristics. Likewise, if the signal and ground electrodes of the RX are unsymmetrical, the RX not only detects the differential signal from the TX, but also picks up the unsymmetrical TX common mode voltage, effectively causing it to function as a capacitive RX.

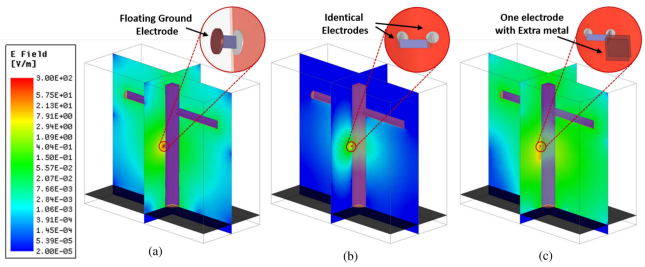

Fig. 6. (a) E-field plot for capacitive EQS-HBC, with the signal electrode attached to the body and the ground electrode floating. (b) E-field plot for symmetrical galvanic EQS-HBC, with both the signal and ground electrodes attached to the body. (c) E-field plot for unsymmetrical galvanic EQS-HBC, where the field distribution exhibits greater similarity to capacitive EQS-HBC than to galvanic EQS-HBC.

VI. Future Directions

As IoB technology advances, the formation of a comprehensive network of on-body devices is enabling more sophisticated applications, some of which require significantly higher data rates—such as high-resolution streaming in smart glasses. While EQS-HBC offers inherent privacy advantages due to its low-frequency operation (<30 MHz) [3], its data rate is fundamentally constrained by these operational frequencies. This limitation has driven substantial research into the resonant-HBC, where higher carrier frequencies can be leveraged to enhance data rates [11], [18].

In resonant-HBC, circuit modeling is still evolving. The key distinction between that and EQS-HBC lies in the need to account for not only the lumped circuit elements identified in EQS-HBC but also the radiative components that emerge as the system transitions from the near-field to the mid-field (Fresnel) region. This introduces additional complexity to the circuit modeling process, as both radiative and conductive behaviors must be integrated to accurately capture the full dynamics of resonant-HBC.

Furthermore, as Sarkar et al. have explored the relationship between AC excitation relaxation time and material electrical properties [34], HBC could potentially be extended beyond the human body to various structures and materials.

VII. Conclusion

This paper reviewed key circuit models for HBC, with a focus on capacitive EQS-HBC and galvanic EQS-HBC. The role of parasitic capacitance in limiting the channel response for capacitive EQS-HBC was analyzed, and the conditions under which an unsymmetrical galvanic EQS-HBC converges to capacitive EQS-HBC were discussed. Additionally, future directions in resonant-HBC were explored. By consolidating these lumped circuit models, this paper offers a foundation for future HBC circuit applications and advancements in wearable communication technologies.

REFERENCES

[1] A. Datta and S. Sen, "Invited: Can Wi-R enable perpetual IoB nodes?" *BioCAS 2023 - 2023 IEEE Biomedical Circuits and Systems Conference, Conference Proceedings*, 2023.

[2] A. Datta and S. Sen, "Invited: IoB: The Vision of the Internet of Bodies," *Midwest Symposium on Circuits and Systems*, pp. 444–448, 2023.

[3] D. Das, S. Maity, B. Chatterjee *et al.*, "Enabling Covert Body Area Network using Electro-Quasistatic Human Body Communication," *Scientific Reports*, vol. 9, no. 1, 12 2019.

[4] S. Maity, D. Das, X. Jiang *et al.*, "Secure Human-Internet using dynamic Human Body Communication," *Proceedings of the International Symposium on Low Power Electronics and Design*, 8 2017.

[5] S. Maity, N. Modak, D. Yang *et al.*, "A 415 nW Physically and Mathematically Secure Electro-Quasistatic HBC Node in 65nm CMOS for Authentication and Medical Applications," *Proceedings of the Custom Integrated Circuits Conference*, vol. 2020-March, 3 2020.

[6] S. Maity, D. Yang, S. S. Redford *et al.*, "BodyWire-HCI: Enabling New Interaction Modalities by Communicating Strictly during Touch Using Electro-Quasistatic Human Body Communication," *ACM Transactions on Computer-Human Interaction*, vol. 27, no. 6, 11 2020.

[7] S. Sen, S. Maity, and D. Das, "The body is the network: To safeguard sensitive data, turn flesh and tissue into a secure wireless channel," *IEEE Spectrum*, vol. 57, no. 12, pp. 44–49, 12 2020.

[8] M. Nath, S. Maity, S. Avlani *et al.*, "Inter-body coupling in electro-quasistatic human body communication: theory and analysis of security and interference properties," *Scientific Reports*, vol. 11, no. 1, 12 2021.

[9] A. Datta and S. Sen, "Physically-secure low-power human state measurement using EQS-HBC and Edge-Analytics : Invited paper," *2021 IEEE Research and Applications of Photonics in Defense Conference, RAPID 2021*, 8 2021.

[10] D. Yang, S. Maity, S. Sen *et al.*, "Physically Secure Wearable–Wearable Through-Body Interhuman Body Communication," *Frontiers in Electronics*, vol. 2, p. 807051, 2 2022. [Online]. Available: www.frontiersin.org

[11] S. Sarkar, Q. Huang, M. Nath *et al.*, "Wearable Human Body Communication Channel Measurements in the Body Resonance Regime," *IEEE MTT-S International Microwave Symposium Digest*, pp. 800–803, 2024.

[12] S. Sen, "SocialHBC: Social Networking and Secure Authentication using Interference-Robust Human Body Communication," *Proceedings of the International Symposium on Low Power Electronics and Design*, pp. 34–39, 8 2016. [Online]. Available: https://dl.acm.org/doi/10.1145/2934583.2934609

[13] X. Jiang and S. Sen, "Secure, energy-efficient, interference-robust connectivity for physiological sensors using human body communication," *Proceedings of the IEEE National Aerospace Electronics Conference, NAECON*, vol. 0, pp. 119–122, 7 2016.

[14] S. Maity, D. Das, and S. Sen, "Adaptive interference rejection in Human Body Communication using variable duty cycle integrating DDR receiver," *Proceedings of the 2017 Design, Automation and Test in Europe, DATE 2017*, pp. 1763–1768, 5 2017.

[15] S. Maity, D. Das, and S. Sen, "Wearable health monitoring using capacitive voltage-mode Human Body Communication," *Proceedings of the Annual International Conference of the IEEE Engineering in Medicine and Biology Society, EMBS*, pp. 1–4, 9 2017.

[16] S. Maity, B. Chatterjee, G. Chang *et al.*, "BodyWire: A 6.3-pJ/b 30-Mb/s-30-dB SIR-Tolerant Broadband Interference-Robust Human Body Communication Transceiver Using Time Domain Interference Rejection," *IEEE Journal of Solid-State Circuits*, vol. 54, no. 10, pp. 2892–2906, 10 2019.

[17] S. Sriram, S. Avlani, M. P. Ward *et al.*, "Electro-Quasistatic Animal Body Communication for Untethered Rodent Biopotential Recording," *Scientific Reports*, vol. 11, no. 1, 12 2021.

[18] Q. Huang, S. Sarkar, and S. Sen, "Enabling Physically Secure Human Body Communication in Body Resonance Region with Faraday Fabric," *2024 IEEE MTT-S International Microwave Biomedical Conference, IMBioC 2024*, pp. 84–86, 2024.

[19] J. Bae, H. Cho, K. Song *et al.*, "The signal transmission mechanism on the surface of human body for body channel communication," *IEEE Transactions on Microwave Theory and Techniques*, vol. 60, no. 3 PART 1, pp. 582–593, 2012.

[20] J. Park, H. Garudadri, and P. P. Mercier, "Channel Modeling of Miniaturized Battery-Powered Capacitive Human Body Communication Systems," *IEEE Transactions on Biomedical Engineering*, vol. 64, no. 2, pp. 452–462, 2 2017.

[21] M. S. Wegmueller, A. Kuhn, J. Froehlich *et al.*, "An attempt to model the human body as a communication channel," *IEEE Transactions on Biomedical Engineering*, vol. 54, no. 10, pp. 1851–1857, 10 2007.

[22] E. Wen, D. Sievenpiper, and P. Mercier, "Channel Characterization of Magnetic Human Body Communication," *IEEE Transactions on Biomedical Engineering*, vol. 69, no. 2, pp. 569–579, 2 2022.

[23] J. F. Zhao, X. M. Chen, B. D. Liang *et al.*, "A Review on Human Body Communication: Signal Propagation Model, Communication Performance, and Experimental Issues," *Wireless Communications and Mobile Computing*, vol. 2017, no. 1, p. 5842310, 1 2017. [Online]. Available: https://onlinelibrary.wiley.com/doi/full/10.1155/2017/5842310

[24] N. Cho, J. Yoo, S. J. Song *et al.*, "The human body characteristics as a signal transmission medium for intrabody communication," *IEEE Transactions on Microwave Theory and Techniques*, vol. 55, no. 5, pp. 1080–1085, 2007.

[25] S. Maity, M. He, M. Nath *et al.*, "Bio-Physical Modeling, Characterization, and Optimization of Electro-Quasistatic Human Body Communication," *IEEE Transactions on Biomedical Engineering*, vol. 66, no. 6, pp. 1761–1802, 6 2019.

[26] M. Nath, S. Maity, and S. Sen, "Toward Understanding the Return Path Capacitance in Capacitive Human Body Communication," *IEEE Transactions on Circuits and Systems II: Express Briefs*, vol. 67, no. 10, pp. 1879–1883, 10 2020.

[27] S. Maity, M. Nath, G. Bhattacharya *et al.*, "On the Safety of Human Body Communication," *IEEE Transactions on Biomedical Engineering*, vol. 67, no. 12, pp. 3392–3402, 12 2020.

[28] S. Maity, K. Mojabe, and S. Sen, "Characterization of Human Body Forward Path Loss and Variability Effects in Voltage-Mode HBC," *IEEE Microwave and Wireless Components Letters*, vol. 28, no. 3, pp. 266–268, 3 2018.

[29] A. Datta, M. Nath, D. Yang *et al.*, "Advanced Biophysical Model to Capture Channel Variability for EQS Capacitive HBC," *IEEE Transactions on Biomedical Engineering*, vol. 68, no. 11, pp. 3435–3446, 11 2021.

[30] N. Modak, M. Nath, B. Chatterjee *et al.*, "Bio-Physical Modeling of Galvanic Human Body Communication in Electro-Quasistatic Regime," *IEEE Transactions on Biomedical Engineering*, vol. 69, no. 12, pp. 3717–3727, 12 2022.

[31] M. N. Nath, A. K. Ulvog, S. Weigand *et al.*, "Understanding the Role of Magnetic and Magneto-Quasistatic Fields in Human Body Communication," *IEEE Transactions on Biomedical Engineering*, vol. 69, no. 12, pp. 3635–3644, 12 2022.

[32] S. Avlani, M. Nath, S. Maity *et al.*, "A 100KHz-1GHz Termination-dependent Human Body Communication Channel Measurement using Miniaturized Wearable Devices," *Proceedings of the 2020 Design, Automation and Test in Europe Conference and Exhibition, DATE 2020*, pp. 650–653, 3 2020.

[33] D. Yang, P. Mehrotra, S. Weigand *et al.*, "In-the-Wild Interference Characterization and Modelling for Electro-Quasistatic-HBC with Miniaturized Wearables," *IEEE Transactions on Biomedical Engineering*, vol. 68, no. 9, pp. 2858–2869, 9 2021.

[34] S. Sarkar, M. Nath, A. Datta *et al.*, "Material property based analysis of Electro-Quasistatic Human-Structure Interactions," *BioCAS 2023 - 2023 IEEE Biomedical Circuits and Systems Conference, Conference Proceedings*, 2023.

[35] T. G. Zimmerman, "Personal area networks: Near-field intrabody communication," *IBM Systems Journal*, vol. 35, no. 3-4, pp. 609–617, 1996.